

# Extragalactic Background Light Inferred from AEGIS Galaxy SED-type Fractions

arXiv:1007.1459

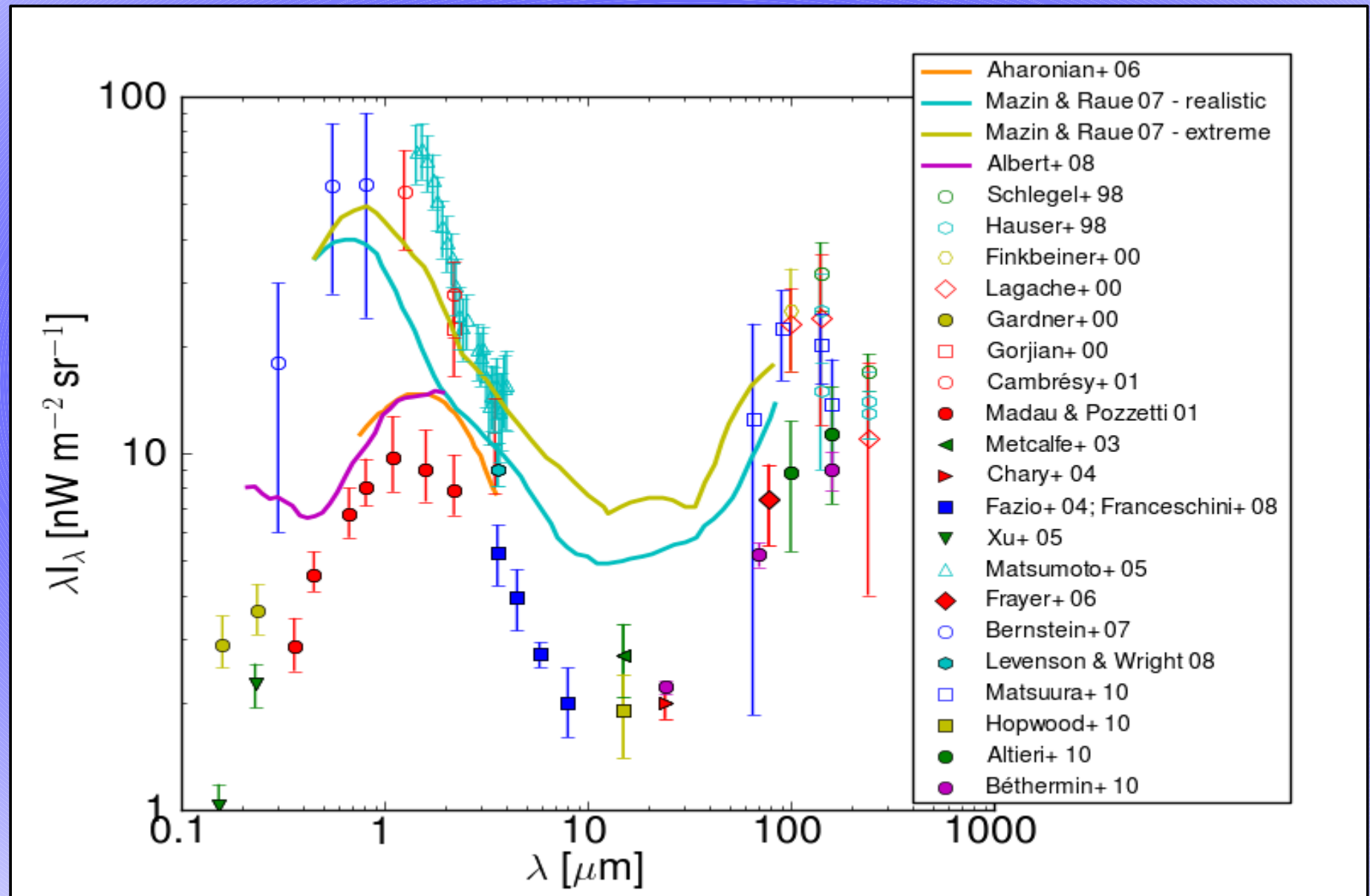
**Alberto Domínguez**  
U. Seville/IAA-Spain  
Visiting student at UCSC

In collaboration with:

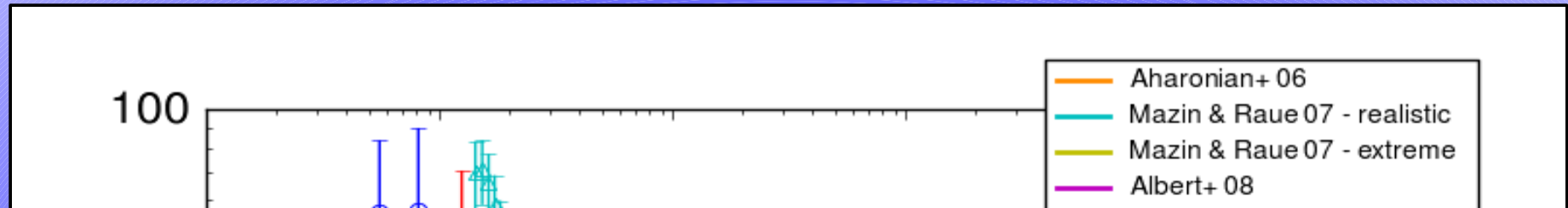
J.R. Primack (UCSC), D.J. Rosario (UCSC), F. Prada (IAA), R.C. Gilmore (SISSA), S.M. Faber (UCSC), D.C. Koo (UCSC), R.S. Somerville (STSI), M. A. Perez-Torres (IAA), P. Perez-Gonzalez (U. Complutense), J. Huang (CfA), M. David (Berkeley), P. Guhathakurta (UCSC), P. Barmby (Western Ontario), C.J. Conselice (Nottingham) and M. Lozano (U. Seville)

UCSC, Santa Cruz, August 20, 2010

# EBL observations



# EBL observations



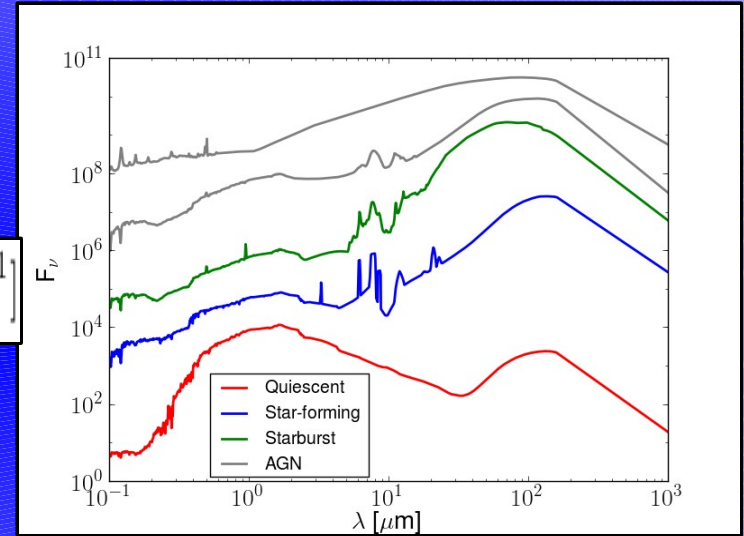
- 1.- Forward evolution, which begins with cosmological initial conditions, apply hypothesis known to be important to galaxy formation, and follows a forward evolution with time, e.g. **Somerville, Gilmore, Primack & Dominguez (in prep)**, and **Gilmore, Somerville, Primack & Dominguez (in prep)**.
- 2.- Backward evolution, which begins with existing galaxy populations and evolves them backwards in time, e.g. Stecker, Malkan & Scully 06; **Franceschini, Rodighiero & Vaccari 08**.
- 3.- Evolution that is directly observed, or inferred, over a range of redshift, e.g. Fardal et al. 07; Finke, Razzaque & Dermer 09; Kneiske & Dole 10; Younger & Hopkins 10. Our model belongs in this category.

λ [μm]

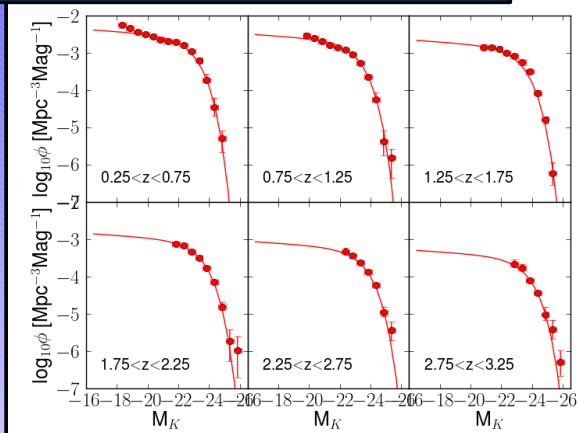
# Methodology

$$\begin{aligned}
 j_i(\lambda, z) &= j_i^{faint} + j_i^{mid} + j_i^{bright} = \\
 &= \int_{M_2=-21.0}^{M_1=-16.6} \Phi(M_K^z, z) f_i T_i(M_K^z, \lambda) (1+z) dM_K^z + \\
 &+ \int_{M_3=-23.0}^{M_2=-21.0} \Phi(M_K^z, z) m_i T_i(M_K^z, \lambda) (1+z) dM_K^z + \\
 &+ \int_{M_4=-25.0}^{M_3=-23.0} \Phi(M_K^z, z) b_i T_i(M_K^z, \lambda) (1+z) dM_K^z
 \end{aligned}$$

Galaxy Spectral Energy Distributions (SEDs)  
SWIRE template library, Polletta+ 07



Luminosity function  
rest-frame K-band, Cirasuolo+ 10



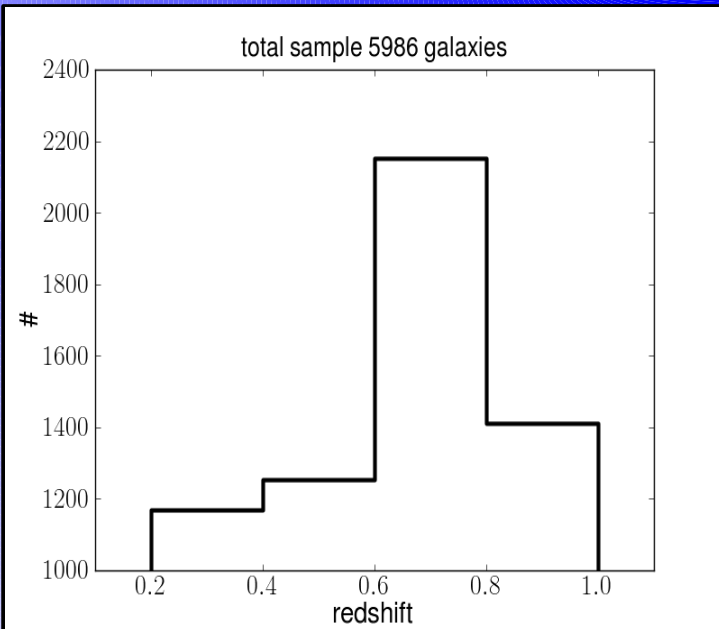
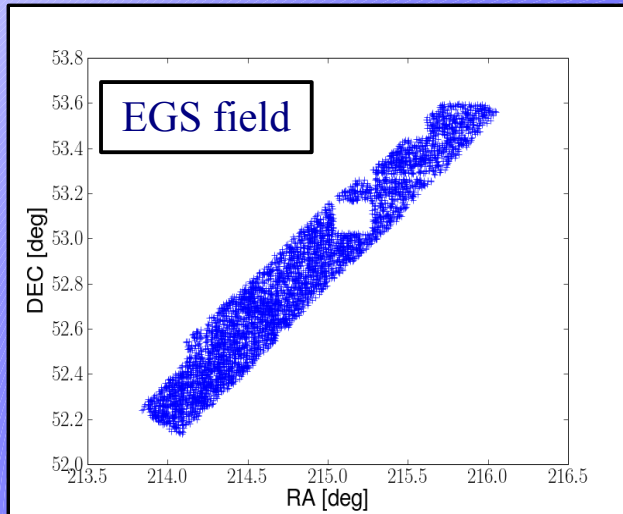
Galaxy SED-type fractions, this work

$$\lambda I_\lambda(\lambda, z) = \frac{c^2}{4\pi\lambda} \int_z^{z_{max}} j_{total}[\lambda(1+z)/(1+z'), z'] \left| \frac{dt}{dz'} \right| dz'$$

EBL spectrum

[nW m<sup>-2</sup> sr<sup>-1</sup>]

# Our galaxy sample from AEGIS



Band	$\lambda_{eff}$ [ $\mu\text{m}$ ]	Observatory	Req.	UL [ $\mu\text{Jy}$ ]
FUV	0.1539	GALEX	ext	-
NUV	0.2316	GALEX	ext	-
<i>B</i>	0.4389	CFHT12K	det	-
<i>R</i>	0.6601	CFHT12K	det	-
<i>I</i>	0.8133	CFHT12K	det	-
<i>K<sub>S</sub></i>	2.14	WIRC	det	-
IRAC 1	3.6	IRAC	det	-
IRAC 2	4.5	IRAC	obs	1.2
IRAC 3	5.8	IRAC	obs	6.3
IRAC 4	8.0	IRAC	obs	6.9
MIPS 24	23.7	MIPS	obs	30

Total: 5986 galaxies

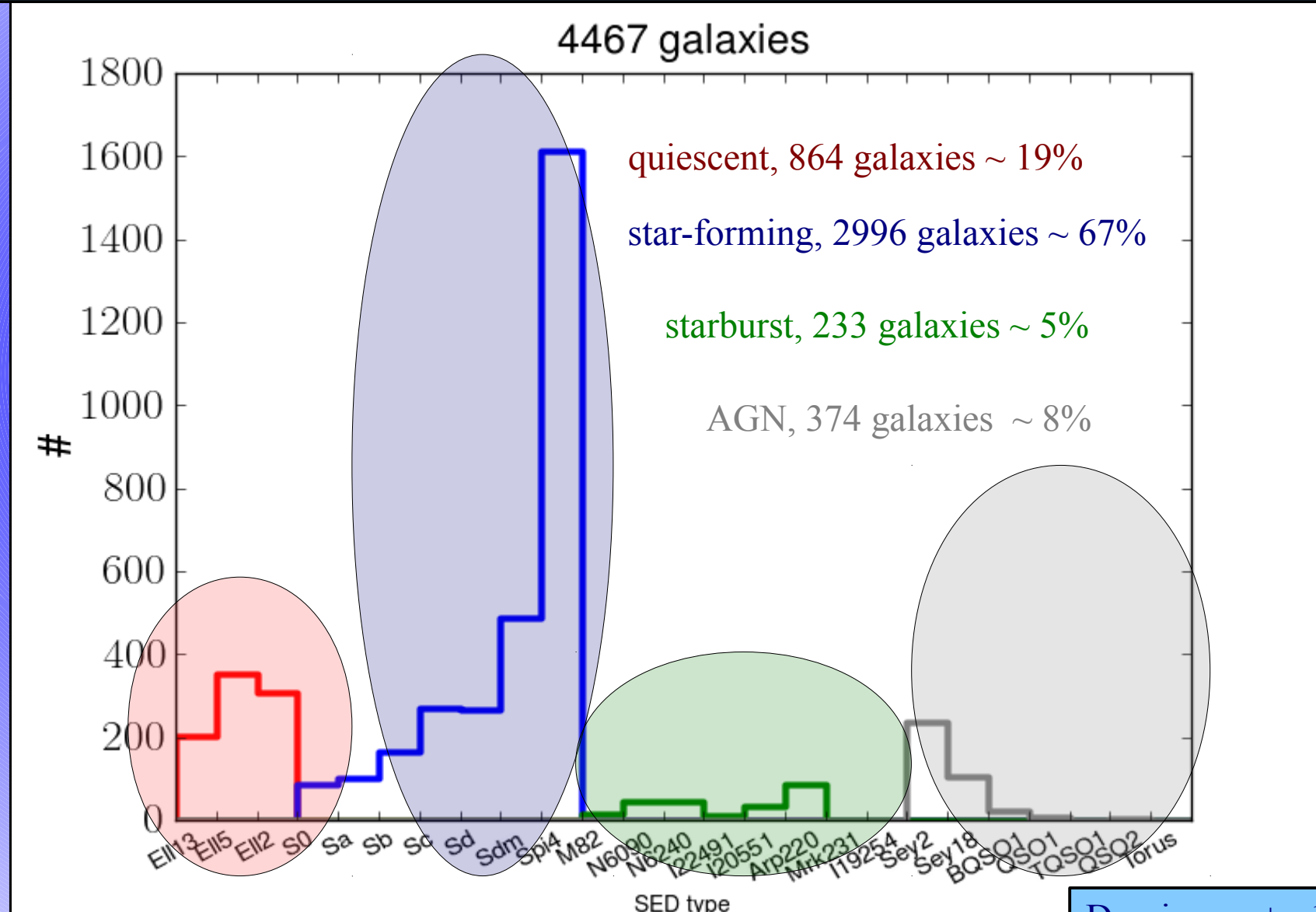
Area: 0.7 sq deg

DEEP2 spectroscopic redshift: 4376 galaxies

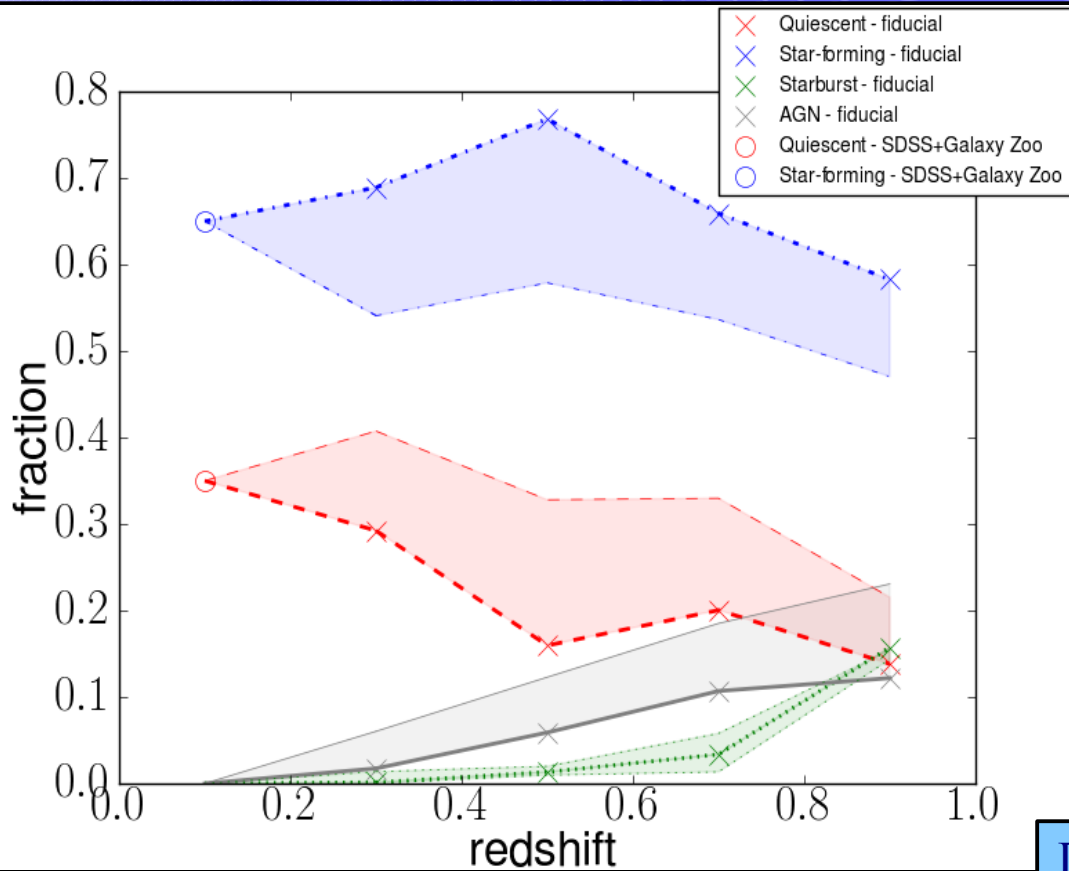
Photometric redshift with mean error less than 0.1: 1610 galaxies

# Chi2 fit

Le PHARE code for fitting the SWIRE templates in FUV, NUV, B, R, I, Ks, IRAC1, 2, 3, 4 and MIPS24



# Galaxy SED-type fractions



Local fractions,  $z < 0.2$ :

Goto+ 03, morphologically classified from Sloan converted to spectral classification using results from Galaxy Zoo

Skibba+ 09 ~6% blue ellipticals

Schawinski+ 09 ~25% red spirals

Results:

35% red-type galaxies

65% blue-type galaxies

Dominguez+ , 10

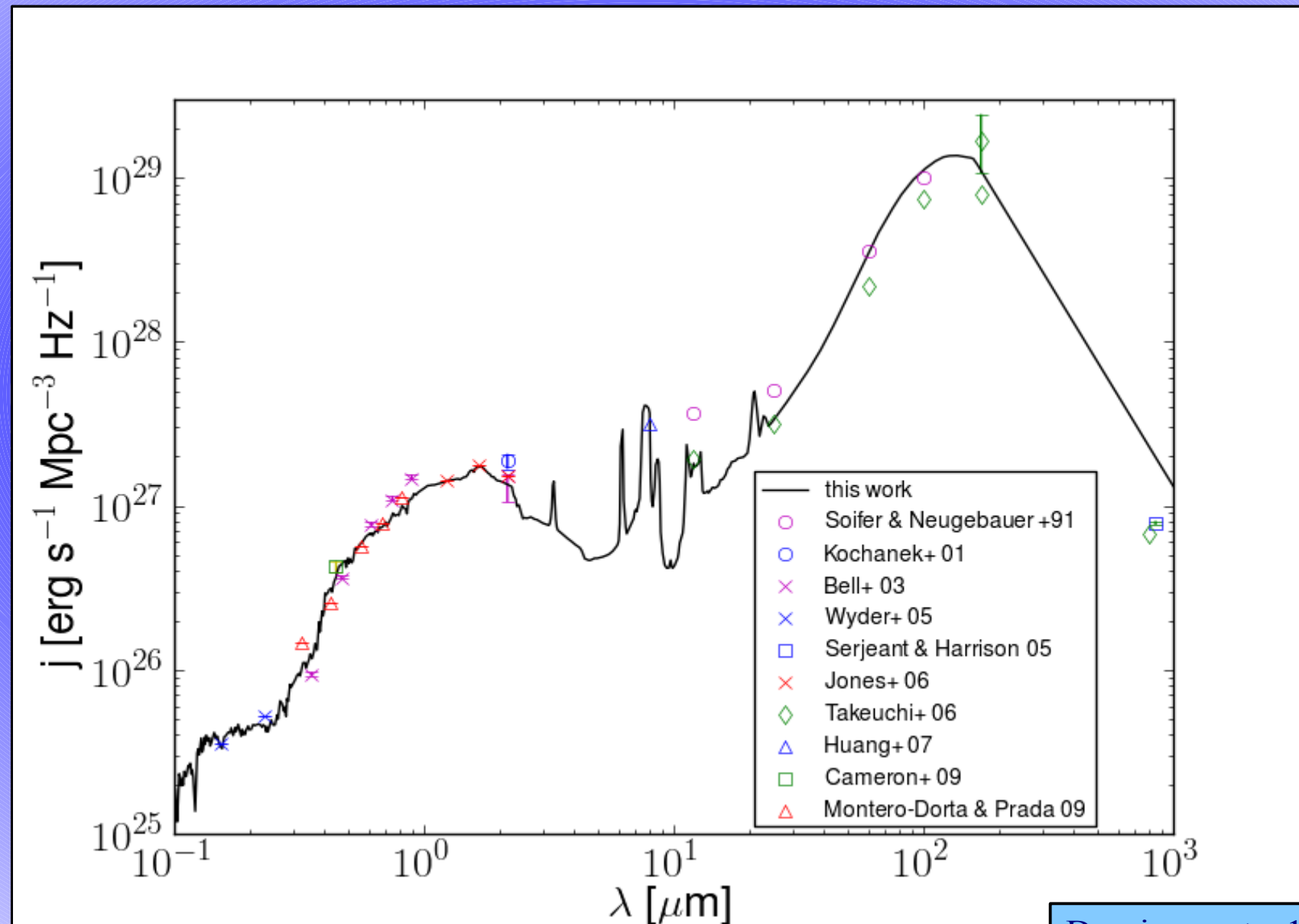
High-redshift universe,  $z > 1$ :

Two approaches:

1.- keep constant the fractions of our last redshift bin

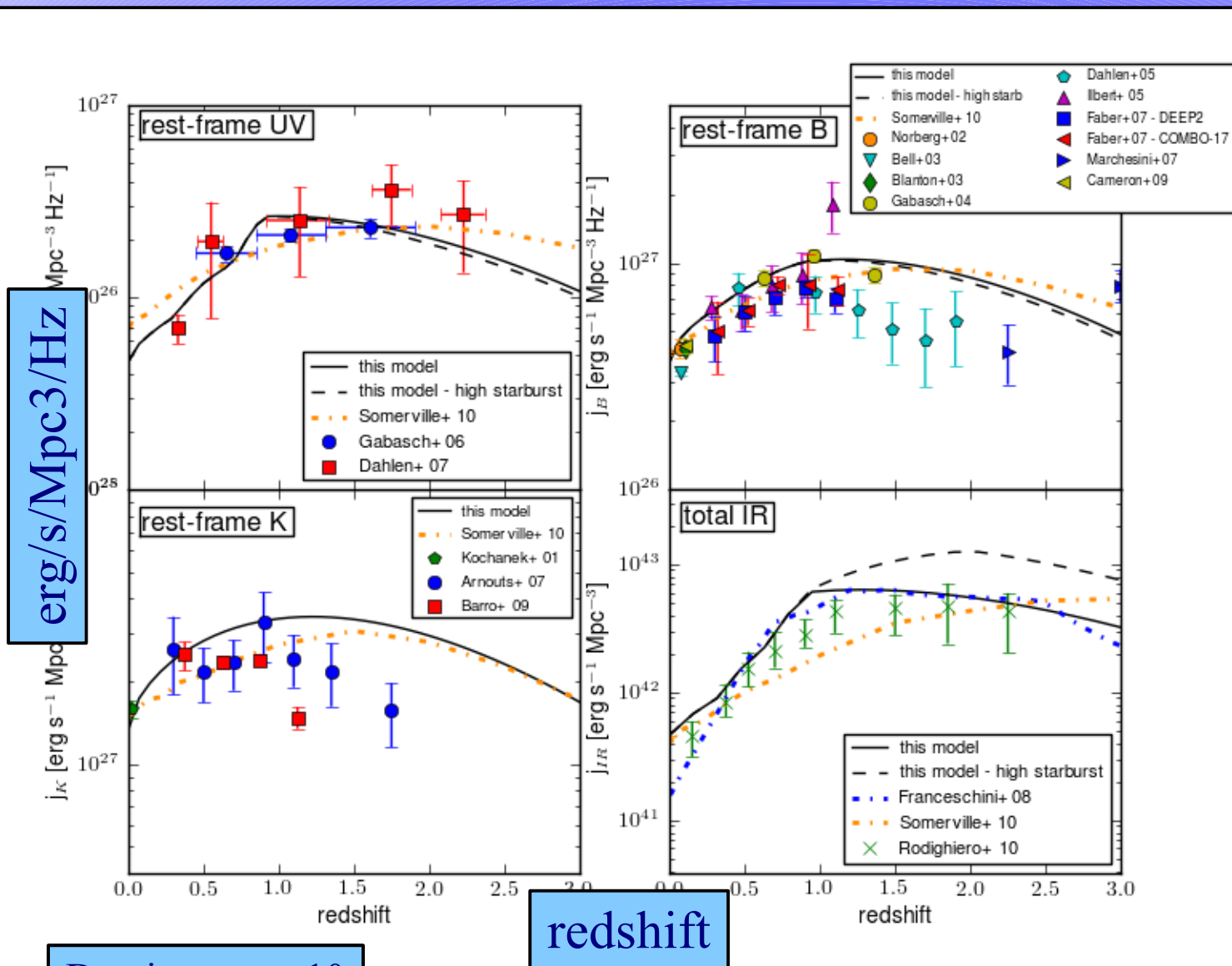
2.- quickly increase starburst population from 16% at  $z=0.9$  to 60% at  $z=2$

# Luminosity densities



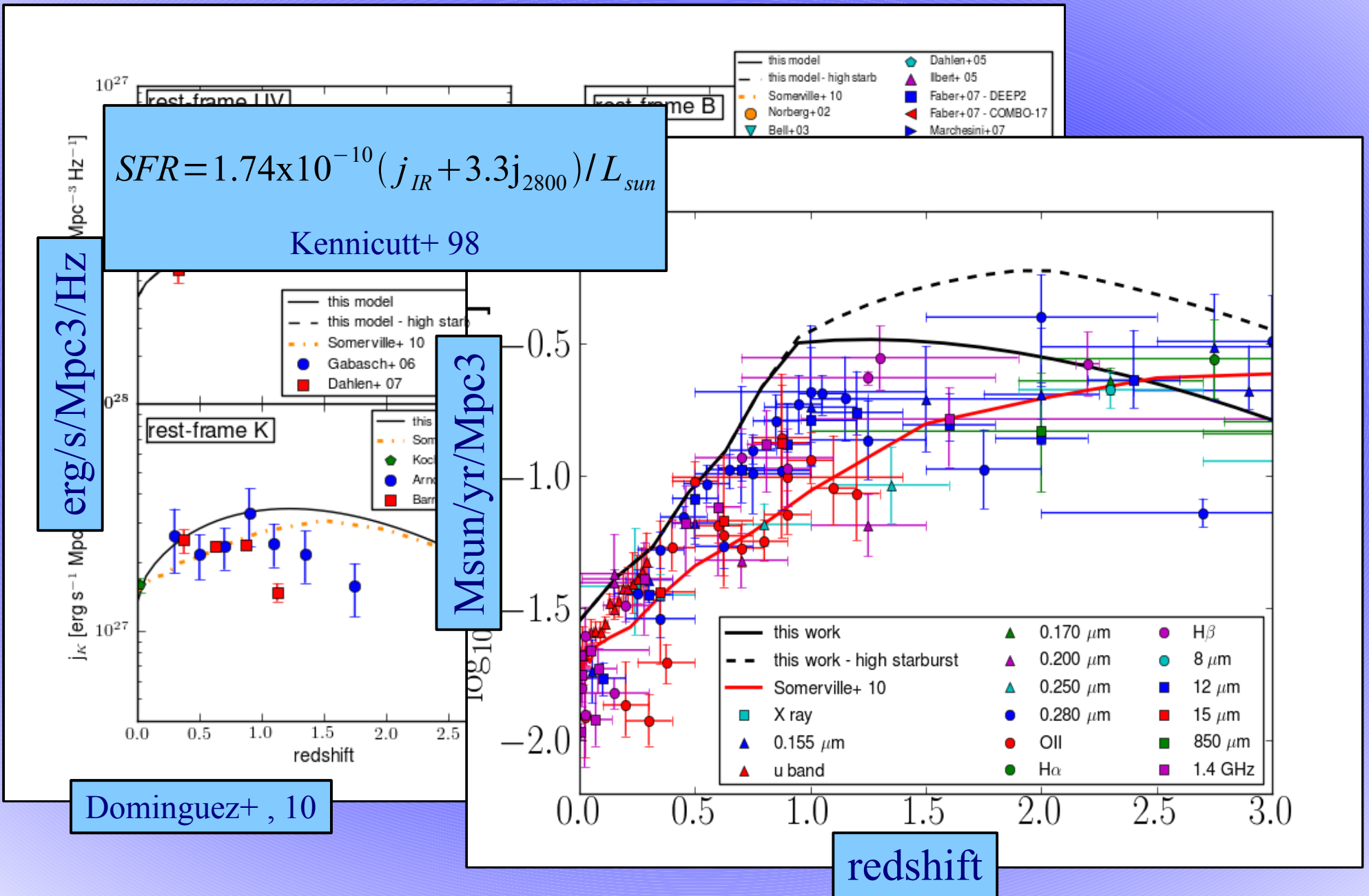


# Luminosity densities and SFR densities



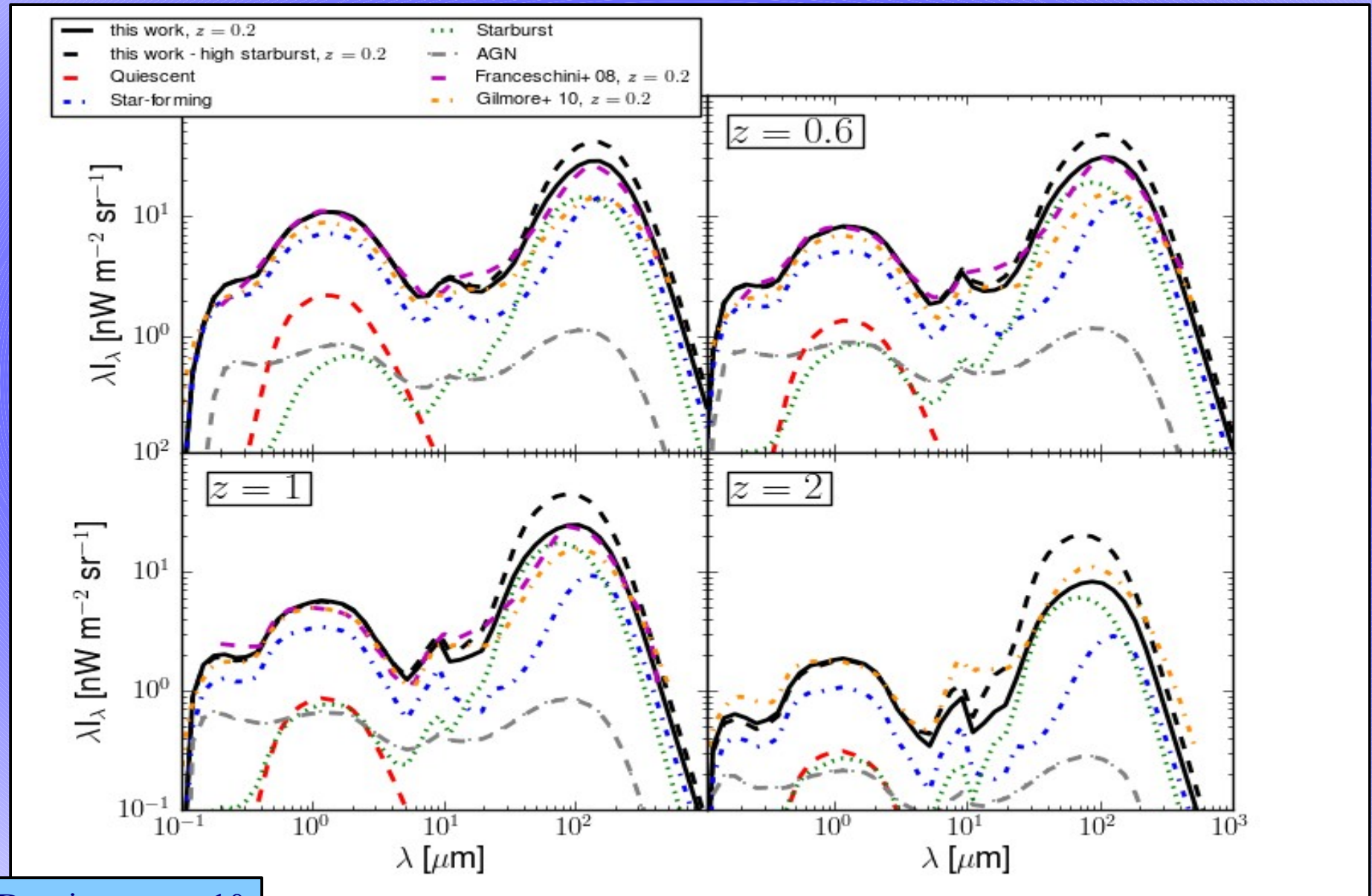
Dominguez+, 10

# Luminosity densities and SFR densities





# EBL history



# Gamma-ray attenuation

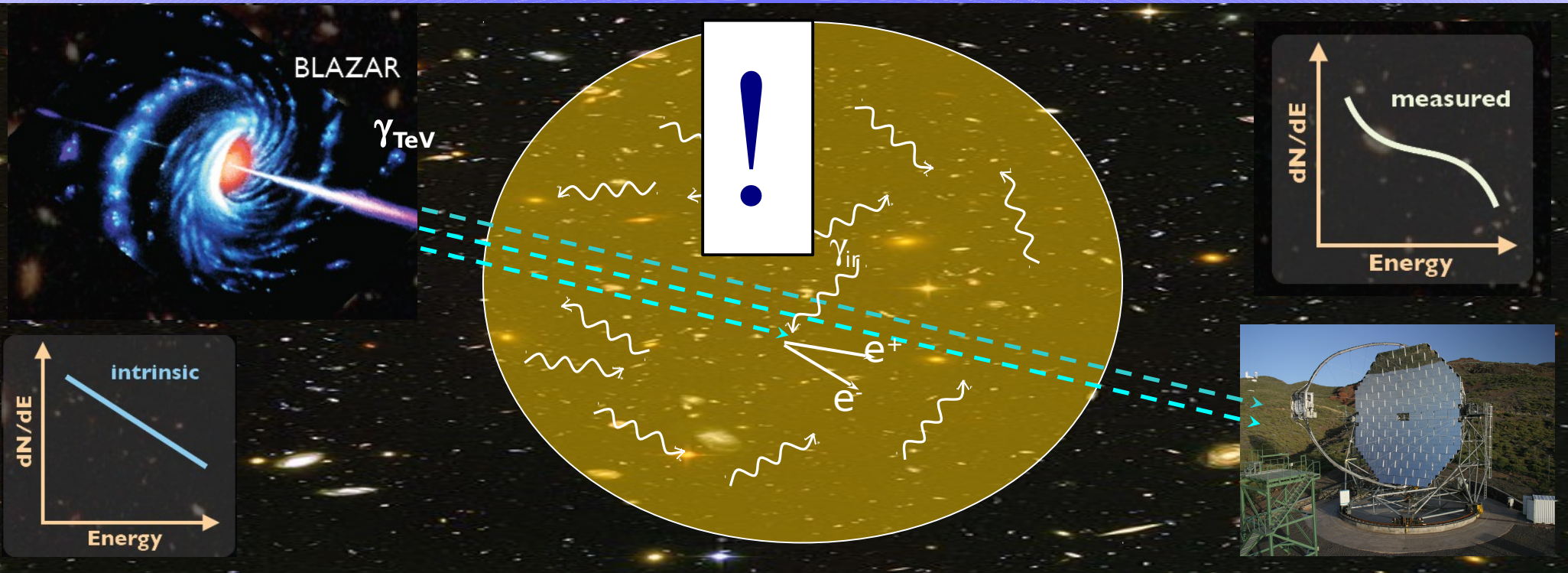


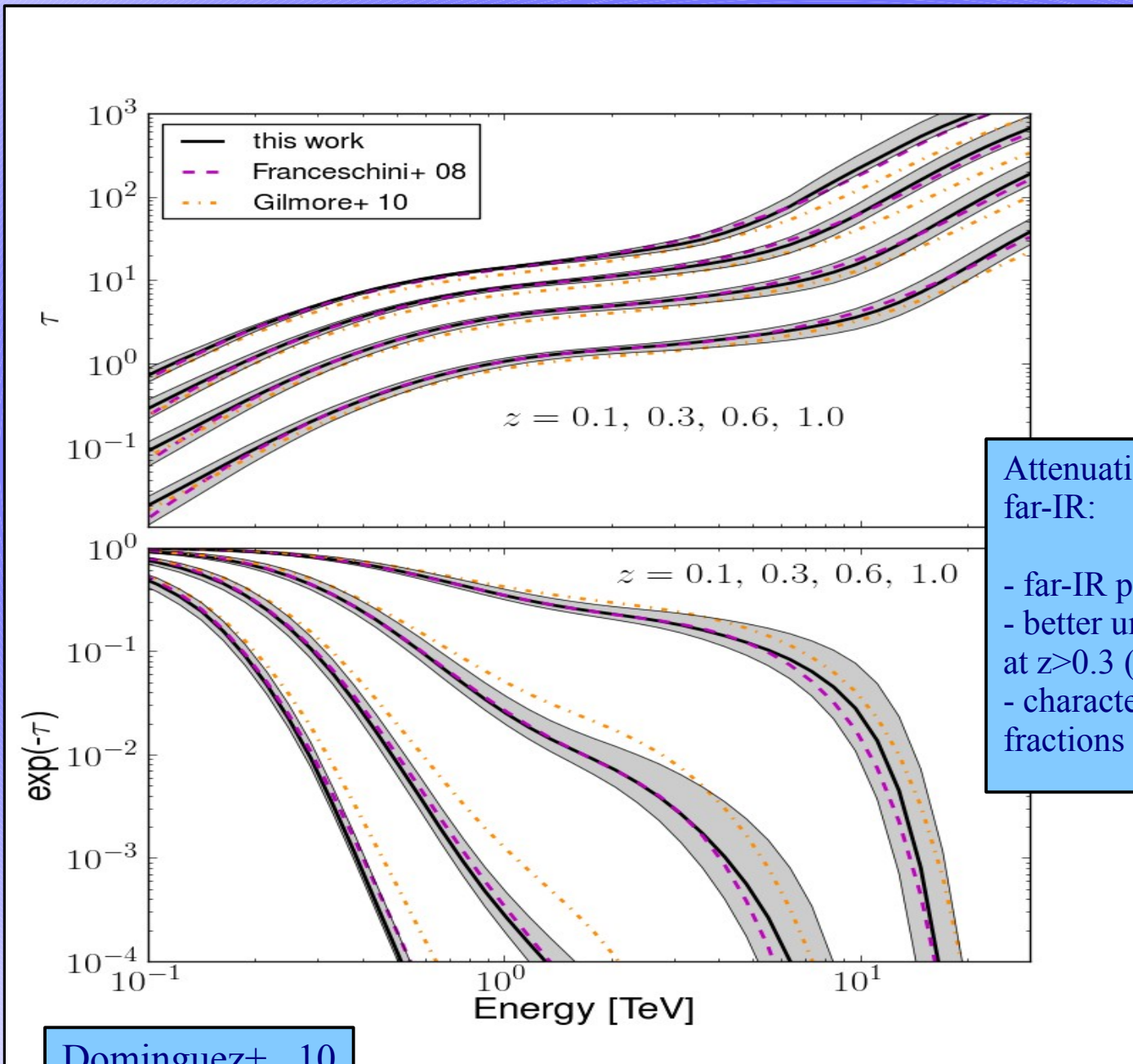
Illustration: D. Mazin & M. Raue

$$\left. \frac{dN}{dE} \right|_{obs} = \left. \frac{dN}{dE} \right|_{int} \exp[-\tau(E, z)]$$



$$\left. \frac{dN}{dE} \right|_{int} = \left. \frac{dN}{dE} \right|_{obs} \exp[\tau(E, z)]$$

# Gamma-ray attenuation



Attenuation uncertainties are still large in the far-IR:

- far-IR photometry (Herschel!)
- better understanding of the far-IR emission at  $z > 0.3$  (Herschel!)
- characterization of galaxy SED-type fractions for  $z > 1$  (WFC3!)

# Summary and conclusions

EBL intensities and optical depths available on-line at:  
**[side.iaa.es/EBL](http://side.iaa.es/EBL)**

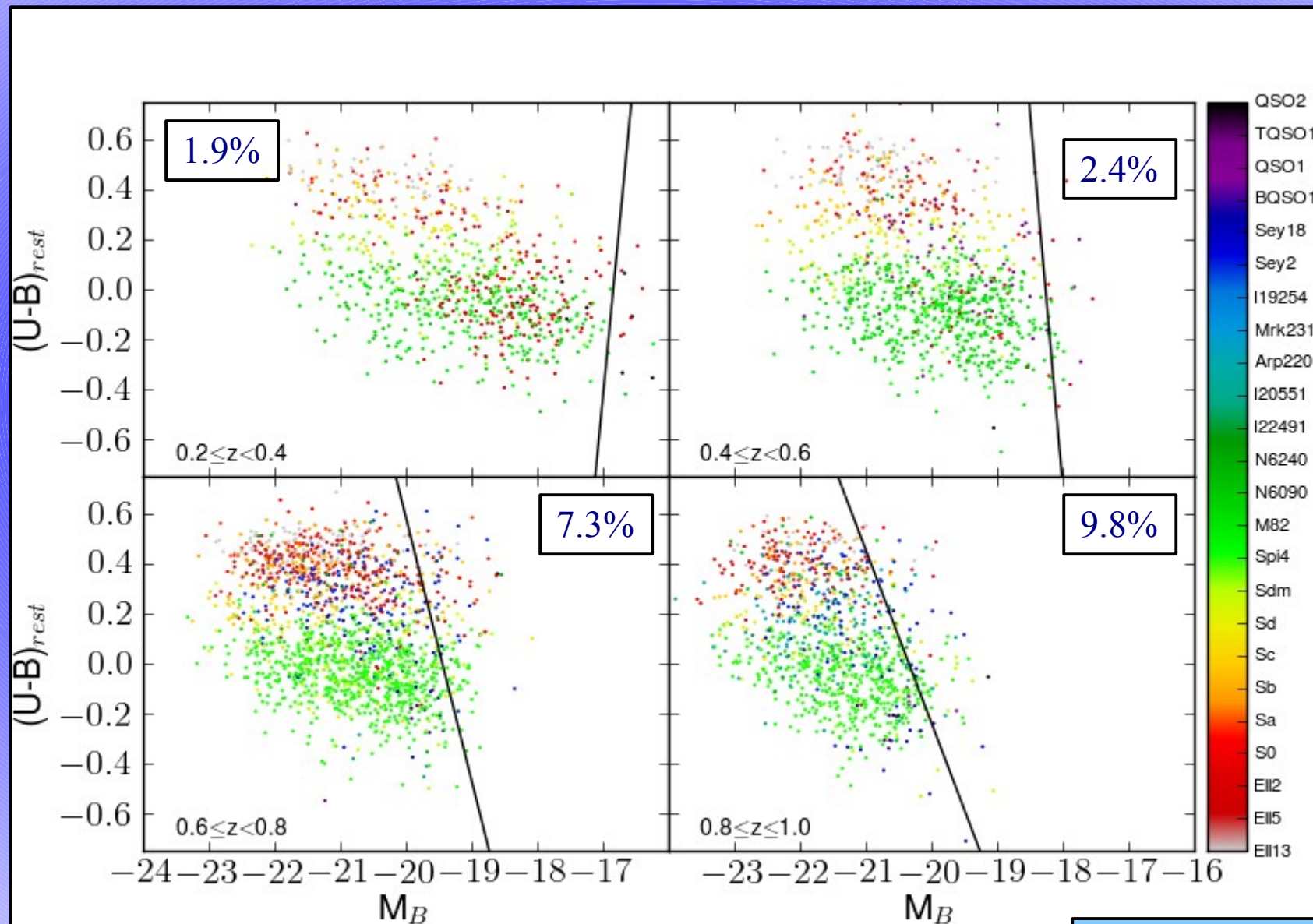
- 1.- Galaxy SED-type fractions from a multi-wavelength catalog of  $\sim 6000$  galaxies between  $z=0.2-1$  from AEGIS.
- 2.- This allows a new calculation of the Extragalactic Background Light (EBL) that uses for the first time galaxy data (LFs and SEDs) over a wide redshift range. We find intensities matching the lower limits from galaxy counts from UV up to mIR, but higher at fIR in agreement with direct measurements. Our model satisfies the limits from gamma-ray astronomy.
- 3.- Study of most of the uncertainties in the modeling. The fIR uncertainties need to be reduced by independent efforts from IR and gamma-ray astronomy. Far-IR photometry, better understanding of galaxy far-IR emission at  $z>0.3$ , galaxy SED-type fractions for  $z>1$  and gamma-ray observations of local sources at  $E>10$  TeV.
- 4.- The semi-analytic approach by Somerville and Gilmore et al. predicts more light (up to a factor  $\sim 2.5$  at some wavelengths) at high redshifts, but less (a factor  $\sim 1.3$ ) at low redshifts than our observational model over all wavelengths.
- 5.- Transparency of the universe to gamma-ray in agreement with Franceschini08 within uncertainties.

EBL intensities and optical depths available on-line at:

[side.iaa.es/EBL](http://side.iaa.es/EBL)



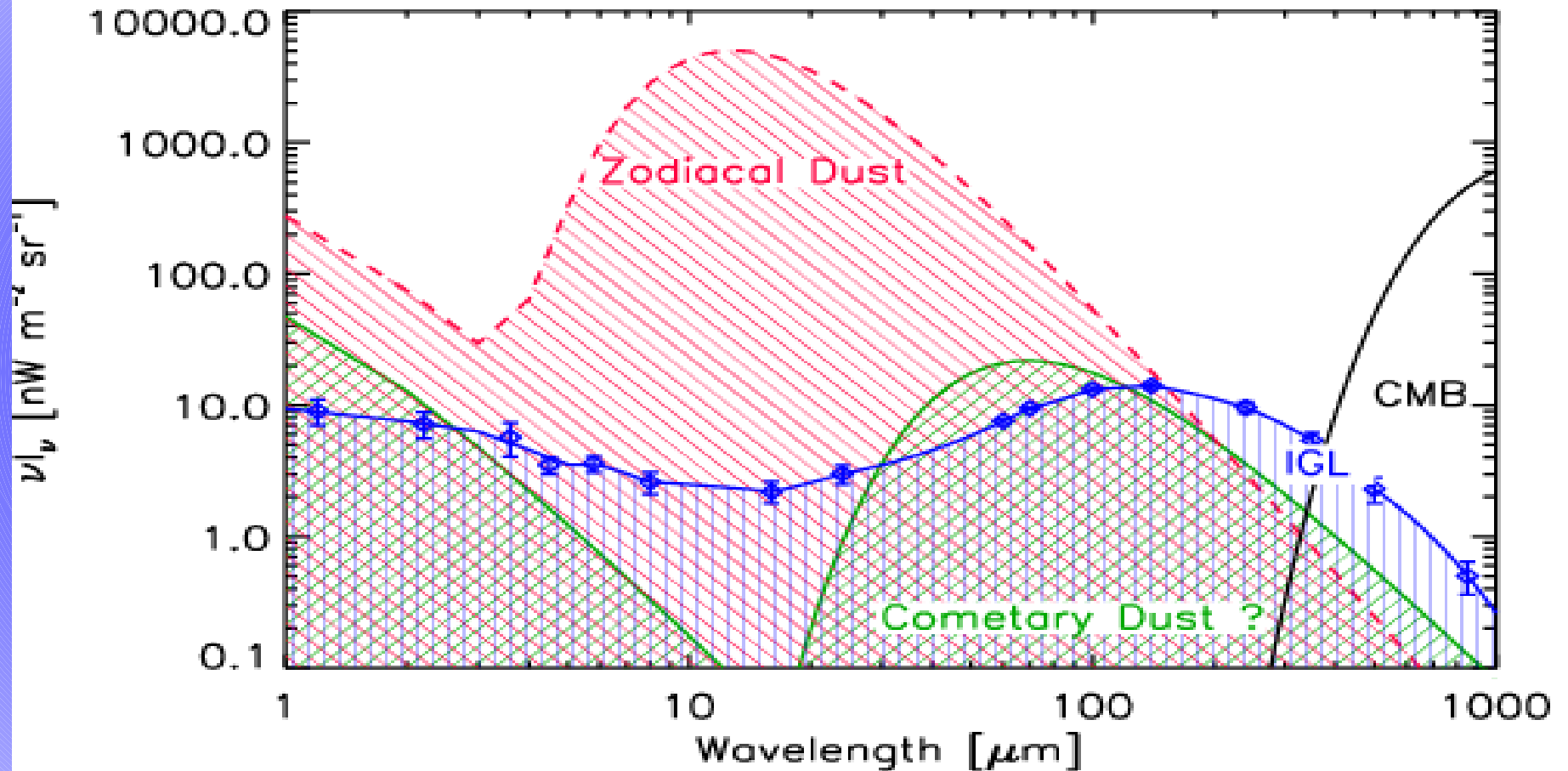
# Color-selection effect



Black-solid line from Willmer+ 06

Dominguez+ , 10

# Supplementary info



# Supplementary info

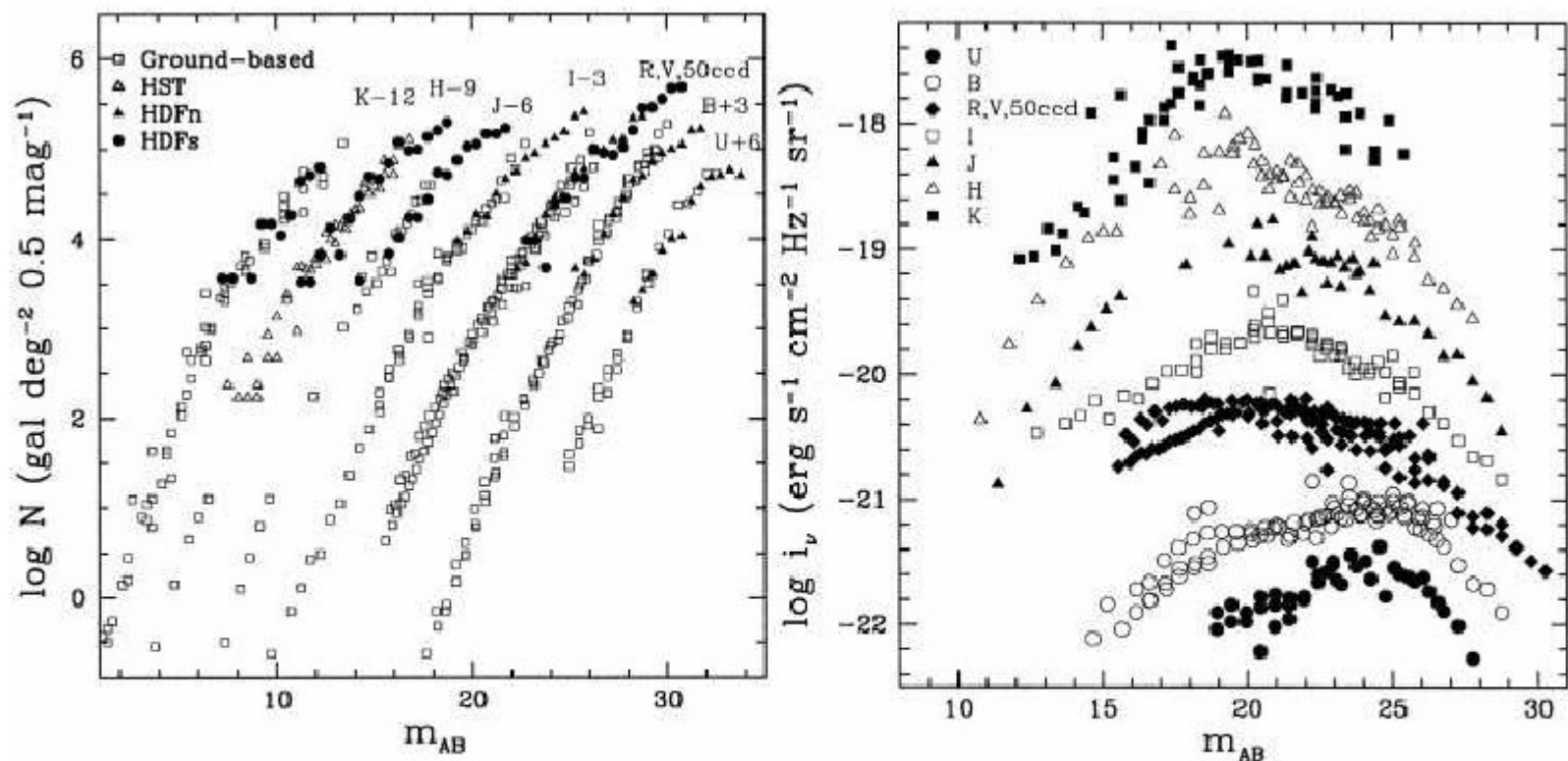
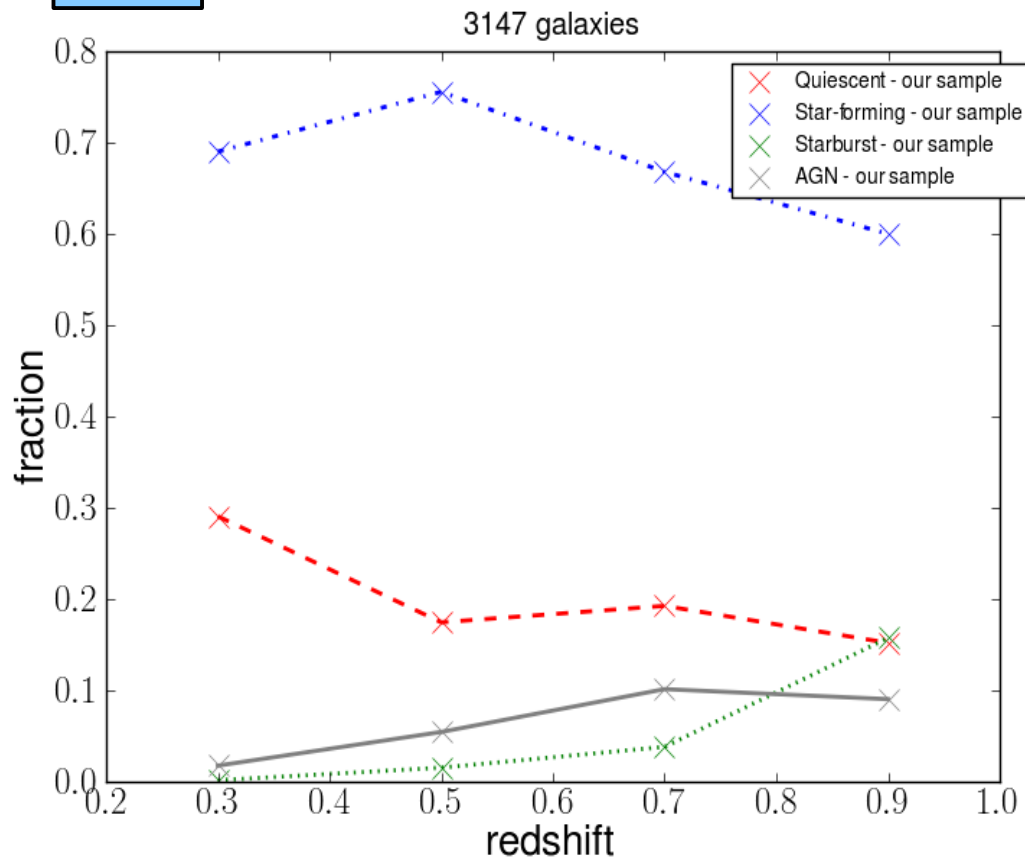


**Figure 1.** *Left:* Differential *UBVIJHK* galaxy counts as a function of AB magnitudes. The sources of the data points are given in the text. Note the decrease of the logarithmic slope  $d \log N/dm$  at faint magnitudes. The flattening is more pronounced at the shortest wavelengths. *Right:* Extragalactic background light per magnitude bin,  $i_\nu = 10^{-0.4(m_{AB}+48.6)}N(m)$ , as a function of *U* (filled circles), *B* (open circles), *V* (filled pentagons), *I* (open squares), *J* (filled triangles), *H* (open triangles), and *K* (filled squares) magnitudes. For clarity, the *BVIJHK* measurements have been multiplied by a factor of 2, 6, 15, 50, 150 and 600, respectively.

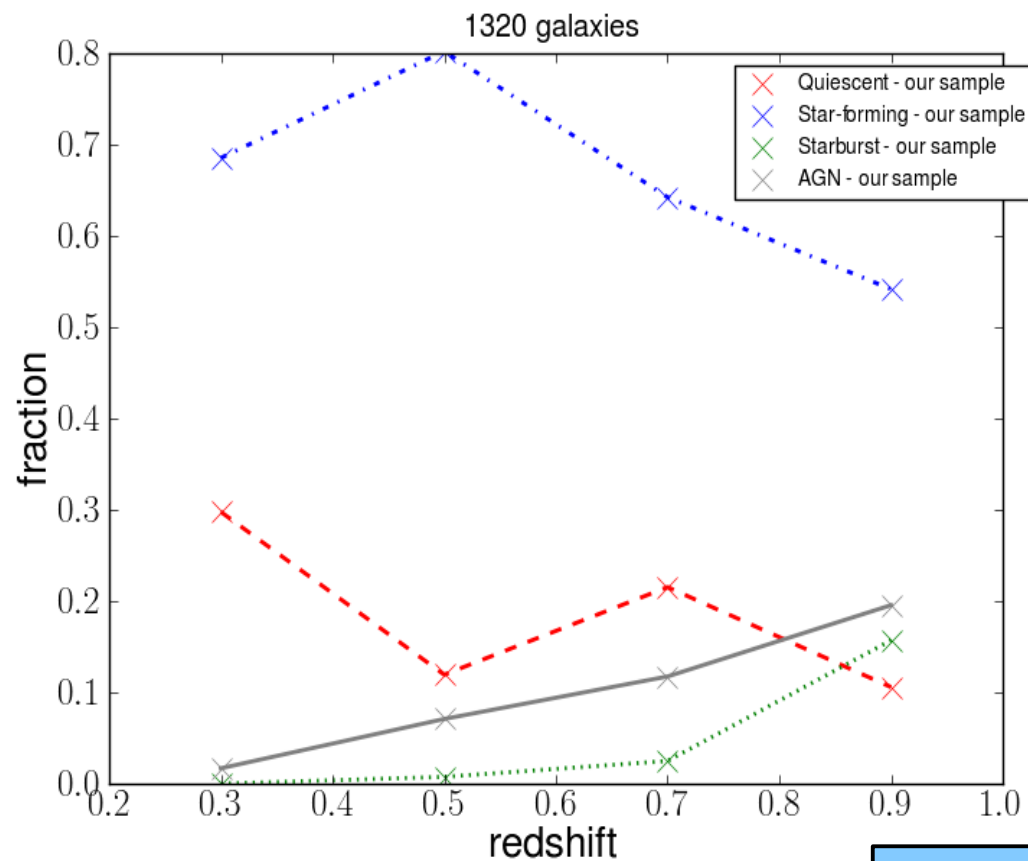
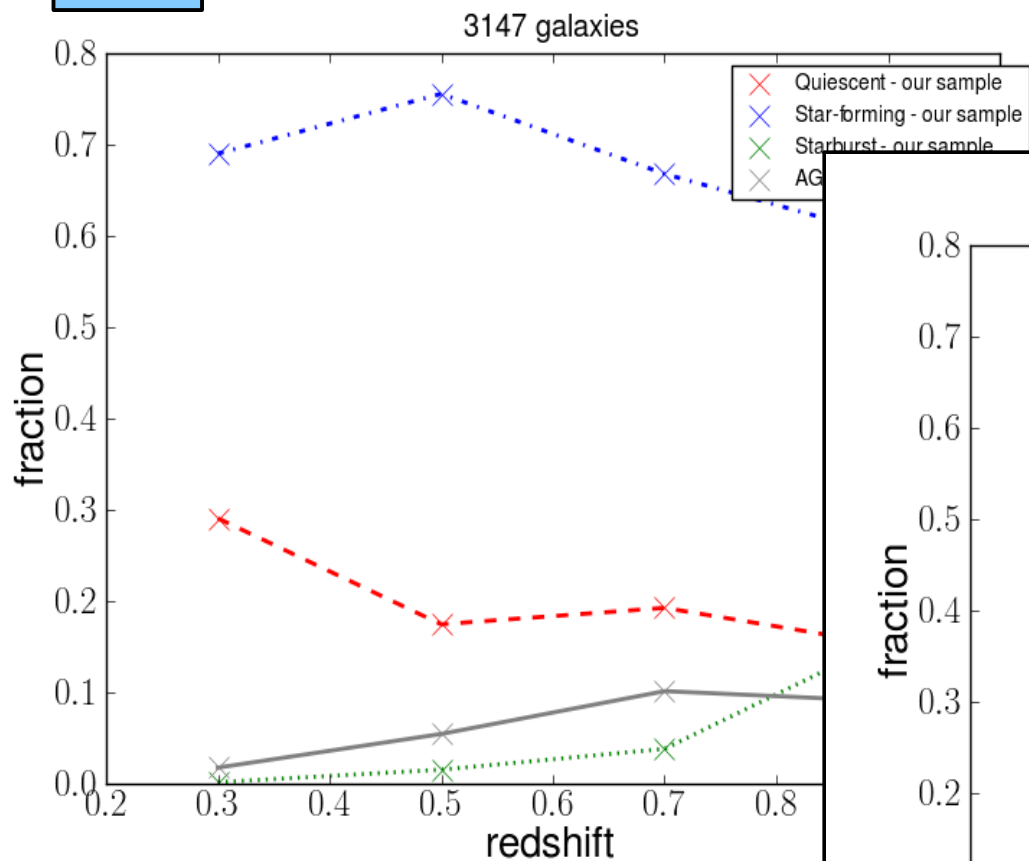
# Supplementary info

specz



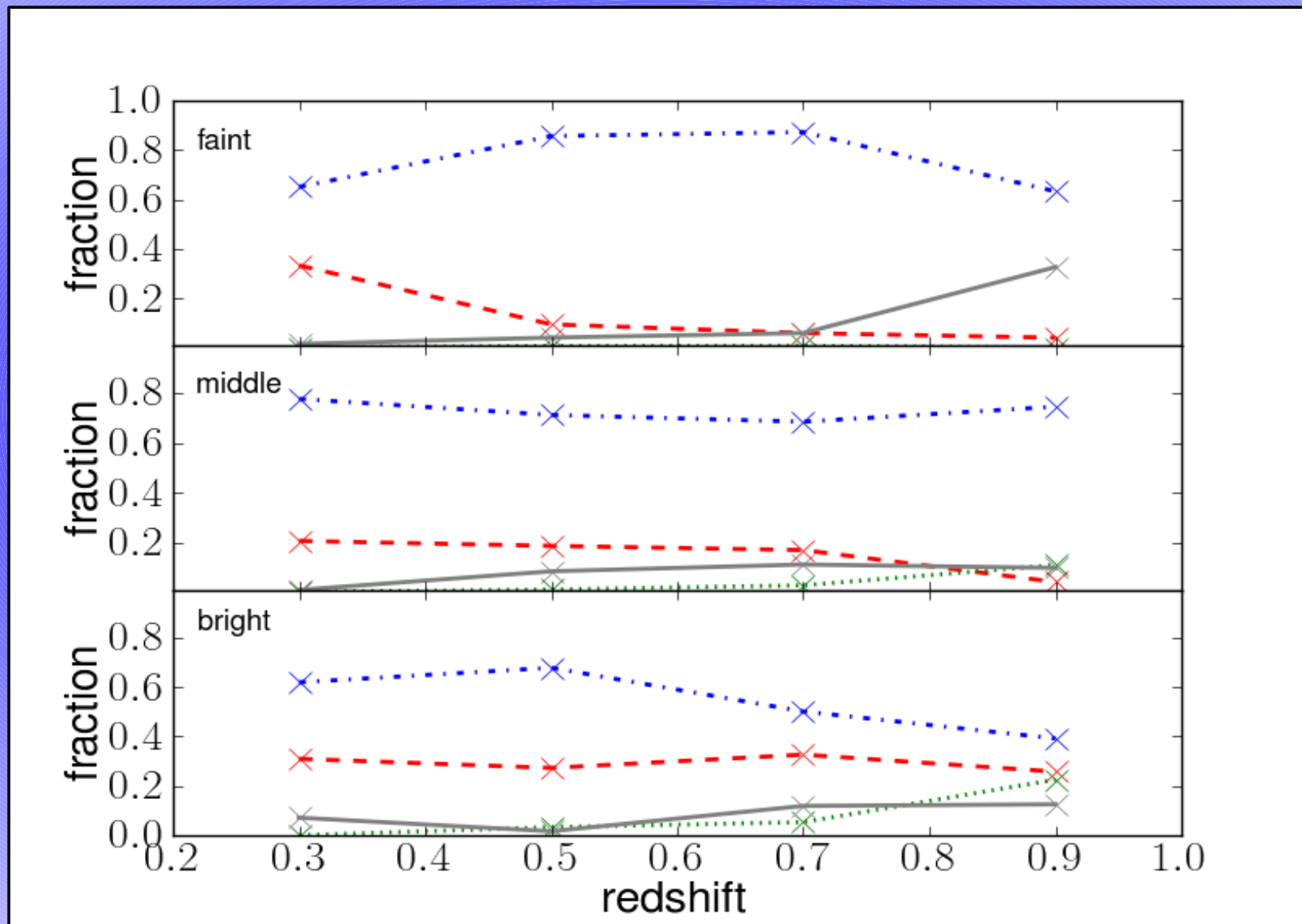
# Supplementary info

specz



photoz

# Supplementary info



# Supplementary info

$$\begin{aligned}f_{quies} &= f_{ell} - (f_{ell} * f_{be}) + (f_{spi} * f_{rs}) = \\ &= 0.14 - (0.14 * 0.057) + (0.86 * 0.25) = 0.35\end{aligned}$$

$$\begin{aligned}f_{sf} &= f_{spi} - (f_{spi} * f_{rs}) + (f_{ell} * f_{be}) \\ &= 0.86 - (0.86 * 0.25) + (0.14 * 0.057) = 0.65\end{aligned}$$

# Supplementary info

$z_{mean}$	Quiescent	Star-forming	Starburst	AGN	Total
0.3	235 (29%)	554 (69%)	1 (0%)	14 (2%)	804
0.5	157 (16%)	756 (77%)	13 (1%)	58 (6%)	984
0.7	328 (20%)	1079 (66%)	55 (3%)	175 (11%)	1637
0.9	144 (14%)	607 (58%)	164 (16%)	127 (12%)	1042



# Supplementary info

$z$	Quiescent	Star-forming	Starburst	AGN	$I_{total}$ [ $\text{nWm}^{-2}\text{sr}^{-1}$ ]
0.0	4.71 (7%)	39.70 (57%)	20.45 (30%)	4.41 (6%)	69.26
0.2	3.86 (5%)	38.96 (54%)	24.54 (34%)	5.25 (7%)	72.60
0.6	2.35 (3%)	31.98 (44%)	31.94 (44%)	5.77 (8%)	72.05
1.0	1.46 (3%)	21.66 (38%)	28.97 (51%)	4.36 (8%)	56.46
2.0	0.51 (3%)	6.46 (36%)	9.87 (54%)	1.34 (7%)	18.18